

Independent yields of Rb, In, and Cs isotopes in the proton-induced fission of ^{232}Th

L. Nikkinen,* B. P. Pathak,† L. Lessard,‡ and I. S. Grant§

Foster Radiation Laboratory, McGill University, Montreal, Quebec, Canada

(Received 2 October 1979)

The relative independent yields of Rb, In, and Cs from the fission of ^{232}Th induced by 20–100 MeV protons have been measured by an on-line mass spectrometer. Total numbers of neutrons emitted per fission event have been deduced from the centroids of these isotopic distributions. The reaction mechanism and charge division process are discussed in terms of equal charge displacement and unchanged charge distribution mechanisms. It is found that the charge division does not depend on the incident proton energy. From a comparison between nearly Gaussian-shaped isotopic distributions of indium, and the asymmetric isotopic distribution of Cs, it is inferred that the total fission cross section includes a significant contribution from low-excitation energy events. This contribution seems to increase with the incident proton energy.

NUCLEAR REACTIONS, FISSION $^{232}\text{Th}(p,f)$, $E_p=29, 59, 75, 97$ MeV: measured independent relative yields of Rb, In, Cs. Deduced total numbers of neutrons emitted in nearly symmetric (In) and asymmetric (Rb-Cs) fission; charge division mechanism.

I. INTRODUCTION

In recent years, considerable work has been done with on-line mass spectrometers¹⁻⁵ to complement the extensive studies undertaken by radiochemical methods⁶⁻⁸ on the fission of the heavy elements induced by protons and heavier projectiles. On-line mass spectrometry allows a very accurate determination of the relative cross sections of production of fission fragments. This method, previously limited to the detection of the alkalis, has recently³ been extended to the isotopes of gallium and indium. It is therefore possible to study the near symmetric (In) and asymmetric (Rb-Cs) fission of the isotopes of uranium and thorium. Results on the fission of ^{238}U have already been published.^{2,3} The purpose of this paper is to present the results of our experiments on the proton-induced fission of ^{232}Th .

Very little has been done by on-line mass spectrometry on the proton-induced fission of this particular isotope. Tracy *et al.*¹ measured the isotopic distributions of Rb and Cs at one proton energy (50 MeV) and compared these results with those obtained on ^{238}U and ^{235}U at similar proton energies. Chaumont⁹ obtained distributions for the same elements at 156 MeV. It was hoped that a systematic study of this reaction at several proton energies could give insight into the reaction mechanisms involved. Of particular interest is the energy dependence of the heavy-mass side of the Cs distribution observed in the two previous experiments. The absence of a similar structure in the complementary Rb distributions could lead one to believe that the Cs structure might be caused by shell effects in the vicinity of $N=82$

neutrons, and not by any reaction mechanism. On the other hand, some structure has been reported in the antimony region,¹⁰ which could not be related to any shell closure effect.

In a previous study³ of the proton-induced fission of ^{238}U , the total number of neutrons (ν_T) deduced from the charge split involving the In fragments was found to be higher compared with the ν_T value obtained from the complementary Rb-Cs pairs. This deviation, which increases as the proton energy gets higher, was interpreted as being due to the larger contribution of low-excitation energy events in the Rb-Cs yields. The structure observed on the heavy-mass side of the Cs distributions might be caused by these low-excitation energy events. The present study of the $^{232}\text{Th}(p,f)$ reaction was undertaken to obtain further information on the reaction mechanism pertaining to these different questions.

II. EXPERIMENTAL METHOD

The mass spectrometer and data collection system were essentially identical to the one described in earlier publications.^{2,3} The ion source¹¹ consisted of a graphite oven (see Fig. 1) containing the target material (ThO_2) deposited on 25 graphite disks of diameter 12.7 mm, thickness 28 mg/cm² and separated by 0.3-mm-thick graphite rings. The average target thickness, per disk, was 4.3 mg/cm². The oven is connected to a "chimney" made from a suitable material (tantalum for separating Rb and Cs, rhenium for In) in which the ionization takes place. The fission fragment elements such as Ga, Rb, In, Os, and Cs are stopped in the graphite disks and then diffuse out through

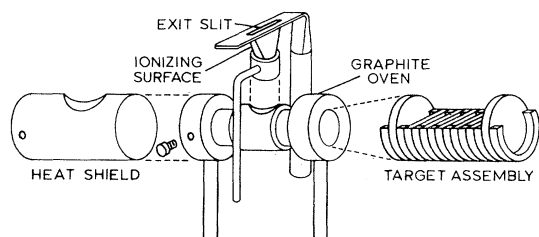


FIG. 1. Ion source used in the present work. The chimney is shown above its fitting place in the ion source.

the chimney where they are selectively ionized, and are finally accelerated through the optics of the mass spectrometer. The oven and ionizer are heated independently by the Joule effect to obtain optimum conditions of source efficiency, diffusion times, and low natural contamination levels.

The irradiations were done in the external beam of the McGill synchrocyclotron. The energy of the beam (100 MeV after extraction) was varied by using beryllium degraders. A bombardment cycle was used, allowing measurement of mass spectra during and after bombardment. The diffusion rates of fission fragments were studied by measuring the yield during and after irradiation in suitably chosen beam on and off cycles. The yield (y) after time t (measured from the end of the irradiation), can be written as a composite of two exponentially decaying components,

$$y = A_1 e^{-\lambda_1 t} + A_2 e^{-\lambda_2 t},$$

where A_1 and A_2 are constants whose values depend on the relative strength of components with diffusion constants λ_1 and λ_2 , respectively. Typical values of A_1 , A_2 , λ_1 , and λ_2 are given in Table I. The observed mass distributions were corrected for diffusion time, decays of radioactive isotopes, and mass discrimination effects. The contribution from the β decays of precursors is expected to be insignificant as the yields of such nuclei are lower by a factor of about 10 as compared to Rb or Cs isotopes of the same mass. The bombardment and data collection cycles were chosen to accept only the fast diffusing component to minimize any contributions from the decay of these precursors.

The mass spectra were collected by modulating

the ion accelerating potential (5 kV) with a triangular sweep. The amplitude of the triangular sweep was adjusted to obtain five masses during the rise time of the sweep and the same five masses during the decay time of the sweep. To cover the whole mass range of interest, measurements were repeated by varying the magnetic field while keeping the sweep range of five masses fixed. For the normalization of measured spectra two consecutive mass ranges were selected to include two overlapping masses. For each beam burst of preset duration, four successive spectra were recorded for equal time intervals, with the first one during the beam burst. The cycle was repeated for several hours to obtain good counting statistics. To determine the relative mass yields the spectrum recorded during the time interval farthest from the beam in time (4th spectrum) was subtracted from the first three to eliminate slow diffusing elements. The results were verified in repeated experiments by using different time cycles of irradiation and data collection after heating the target oven at $\sim 1600^\circ\text{C}$ for several weeks.

III. RESULTS AND DISCUSSION

A. Rb, In, and Cs yields

The relative independent yields of the In isotopes are given in Table II and shown in Fig. 2. Since there are no absolute cross sections available for normalization in this mass region, only relative yields are presented. The fission yields given in Table II have been normalized to a total cross section of 100.0 at each energy. Similar measurements, in the case of the $^{238}\text{U}(p,f)$ reaction, indicate that the total cross section for indium production is comparable, although slightly smaller, to the cesium cross section. An approximate cross section for In yields can therefore be estimated by comparing the total cross sections for In and Cs.

The relative yields of rubidium isotopes were normalized to absolute cross sections by using the reported cross section of ^{92}Y by McGee *et al.*⁸ who used radiochemical methods. These cross sections were extrapolated to rubidium assuming equal cross sections for equal $\langle N/Z \rangle$ values. At 29 MeV, the Rb distribution was normalized so as

TABLE I. Diffusion parameters.

Element	Weight (A_1)	$\tau(1) = \frac{\ln 2}{\lambda(1)}$ (sec)	Weight (A_2)	$\tau(2) = \frac{\ln 2}{\lambda(2)}$ (sec)
Rb	0.62 ± 0.03	0.119 ± 0.004	0.38 ± 0.01	0.84 ± 0.01
Cs	0.57 ± 0.03	0.16 ± 0.01	0.43 ± 0.01	1.55 ± 0.03
In	0.92 ± 0.02	0.045 ± 0.001	0.076 ± 0.002	0.33 ± 0.01

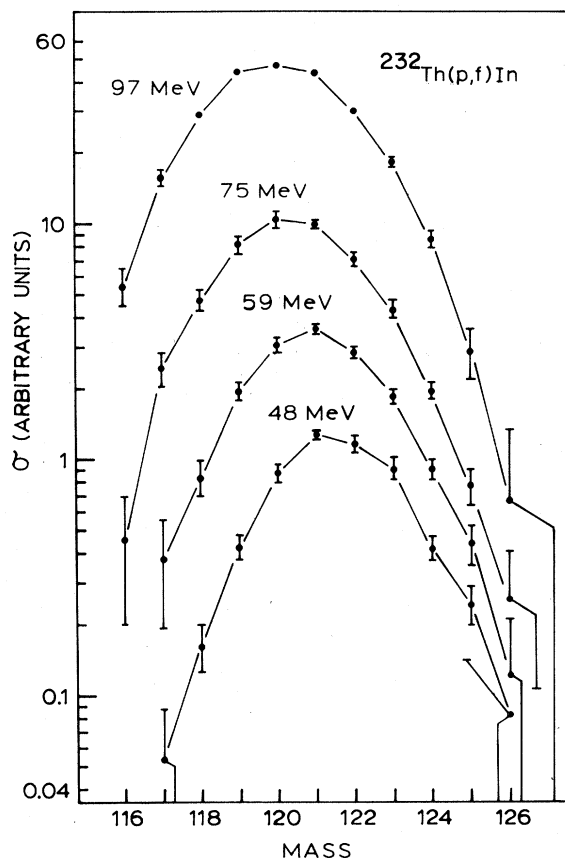
TABLE II. Independent yield of In isotopes in arbitrary units.^a

Mass	97 MeV	75 MeV	59 MeV	48 MeV
116	2.2±0.4	0.9±0.5		
117	6.5±0.4	4.9±0.8	2.4±1.2	0.9±0.6
118	12.0±0.5	9.5±1.0	5.3±0.9	2.9±0.7
119	18.1±0.6	16.1±1.4	12.3±1.1	7.6±0.9
120	19.2±0.6	20.5±1.6	19.1±1.4	15.5±1.4
121	17.7±0.4	19.6±0.9	22.4±0.8	22.8±0.9
122	12.2±0.5	14.0±1.0	17.8±0.9	20.7±1.6
123	7.4±0.3	8.6±0.7	11.5±0.7	16.3±1.7
124	3.5±0.3	3.9±0.3	5.7±0.6	7.4±0.8
125	1.2±0.3	1.5±0.3	2.7±0.5	4.3±0.8
126		0.5±0.3	0.7±0.6	1.5±1.0

^a Normalized to a total cross section of 100.0 at each energy.

to have the same area as that of the 50 MeV data of Tracy *et al.*¹ This was done to avoid the possibility of large error associated with the cross section of ⁸⁷Rb extrapolated from the ⁹²Y cross section. When normalized in this manner, the total Rb cross section was equal to the total Cs cross section at the same energy. The 97 MeV distribution was normalized likewise, by using the 75 MeV distribution because no absolute cross section of ⁹²Y was available at the former energy. The results are summarized in Table III and illustrated in Fig. 3.

The observed isotopic distributions of Cs for 29, 59, and 75 MeV proton energies were normalized at mass 134, 136, and 138 to the data of Benjamin *et al.*⁷ The distribution for 97 MeV data was normalized by assuming the total cross section to be the same as obtained for the 75 MeV incident proton energy. These results are pre-

FIG. 2. Relative independent yields of indium isotopes produced in the ²³²Th(*p,f*)In reaction.

sented in Table IV and Fig. 4 together with the 50 MeV data of Tracy *et al.*¹ and the 156 MeV values of Chaumont⁹ (renormalized by area to the 97 MeV data).

TABLE III. Independent yield (mb) of Rb isotopes.

Mass	156 MeV ^a	97 MeV	75 MeV	59 MeV	50 MeV ^b	29 MeV
84		0.036±0.021				
85	1.20 ±0.10	0.34 ±0.04	0.14±0.03	0.11±0.08	0.06 ±0.03	
86	2.37 ±0.08	1.42 ±0.04	0.72±0.04	0.34±0.03	0.30 ±0.03	
87	5.02 ±0.12	4.75 ±0.15	3.38±0.16	2.2 ±0.2	1.43 ±0.06	0.08±0.7
88	7.50 ±0.22	9.3 ±0.2	7.9 ±0.2	6.3 ±0.4	4.52 ±0.08	3.6 ±0.6
89	10.46 ±0.18	14.4 ±0.2	14.0 ±0.2	13.0 ±0.2	8.77 ±0.06	12.7 ±0.7
90	11.90 ±0.17	17.7 ±0.2	18.6 ±0.2	19.3 ±0.2	12.84 ±0.02	24.5 ±0.9
91	11.65 ±0.15	19.6 ±0.2	21.2 ±0.3	23.4 ±0.4	14.51 ±0.06	37.8 ±1.2
92	8.00 ±0.11	13.6 ±0.1	14.8 ±0.1	16.6 ±0.3	10.80 ±0.11	34.2 ±0.8
93	4.90 ±0.07	8.38 ±0.15	9.4 ±0.3	9.9 ±0.6	6.39 ±0.07	25.7 ±2.0
94	1.91 ±0.04	3.22 ±0.06	3.5 ±0.2	3.7 ±0.2	2.35 ±0.04	10.8 ±1.1
95	0.817±0.03	1.27 ±0.05	1.21±0.13	1.6 ±0.2	0.89 ±0.02	3.6 ±1.1
96	0.195±0.014	0.28 ±0.03	0.31±0.18	0.41±0.24	0.210±0.008	1.7 ±1.4
97	0.061±0.014	0.14 ±0.04	0.24±0.16		0.54 ±0.005	

^aJ. Chaumont (Ref. 9).

^bB. L. Tracy *et al.* (Ref. 1).

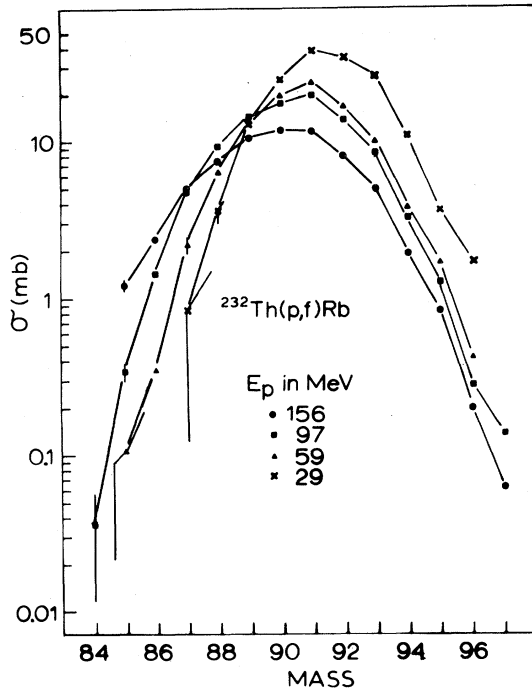


FIG. 3. Independent yields of Rb isotopes produced in the $^{232}\text{Th}(p,f)\text{Rb}$ reaction. Data for 156 MeV proton beam are taken from Chaumont (Ref. 9).

B. Moment analysis of the distributions

The measured isotopic distributions have been analyzed in terms of moments without assuming any functional form for the shape of the distributions. The results of that analysis are summarized in Table V. The errors are the statistical errors

derived from the counting statistics. Figure 5 shows the evolution of the centroids in units of $\langle N/Z \rangle$ as a function of proton energy. It can be seen that the Rb and Cs centroids fall on parallel lines whereas the In values have a strong energy dependence.

The first moments are used to calculate the total numbers of neutrons emitted, for the charge splits yielding the Rb-Cs pair and the In fragments. In the calculation of ν_T , we have assumed that the N/Z ratios of the centroids do not differ significantly for small changes in Z , i.e.,

$$\nu_T = 233 - \langle A \rangle_{\text{Rb}} - \frac{54}{55} \langle A \rangle_{\text{Cs}},$$

$$\nu_T = 233 - \frac{36}{37} \langle A \rangle_{\text{Rb}} - \langle A \rangle_{\text{Cs}},$$

ν_T for Rb-Cs and

$$\nu_T = 233 - \frac{91}{49} \langle A \rangle_{\text{In}},$$

ν_T for In.

The values of ν_T obtained for the two charge splits are given in Table VI, and their variations with proton energy are shown in Fig. 6. The interesting feature, which has also been observed in the proton-induced fission of ^{238}U ,³ is that ν_T (In) diverges more and more from ν_T (Rb-Cs) at proton energies above 40 MeV. The difference in total number of neutrons amounts to ~ 2 at 100 MeV. It has been argued by Chan *et al.*³ that this divergence at higher proton energies is strongly reminiscent of the expected energy dependence of the direct reaction cross section relative to the compound nucleus formation cross section. In-

TABLE IV. Independent yield (mb) of Cs isotopes.

Mass	156 MeV ^a	97 MeV	75 MeV	59 MeV	50 MeV ^b	29 MeV
127	0.029±0.008					
128	0.088±0.008					
129	0.262±0.010					
130	0.557±0.013	0.43±0.12				
131	1.08 ±0.015	1.24±0.16	0.58±0.30			
132	1.63 ±0.03	3.0 ±0.3	1.3 ±0.3	0.54±0.19	0.45±0.04	
133	2.32 ±0.04	7.9 ±0.9	4.5 ±0.7	2.7 ±0.3	1.41±0.08	
134	2.68 ±0.04	9.4 ±0.8	7.8 ±0.9	6.0 ±0.5	4.78±0.18	
135	2.94 ±0.025	11.0 ±1.0	12.3 ±0.8	12.2 ±0.7	11.8 ±0.3	
136	2.86 ±0.03	12.2 ±1.0	13.8 ±0.9	17.5 ±0.8	18.9 ±0.2	5.4±6.4
137	3.14 ±0.05	13.0 ±1.2	16.0 ±1.0	20.2 ±0.9	(21.8)	20.7±7.4
138	2.25 ±0.045	9.8 ±1.2	10.8 ±1.0	14.4 ±0.7	21.2 ±0.4	25.6±7.6
139	2.11 ±0.025	9.2 ±0.5	9.3 ±0.6	12.5 ±0.5	14.8 ±0.3	36.6±6.0
140	1.51 ±0.04	6.9 ±0.7	7.0 ±1.0	8.4 ±0.8	9.0 ±0.3	29.5±5.8
141	1.11 ±0.03	5.0 ±0.6	5.6 ±0.9	5.8 ±0.7	5.9 ±0.2	21.2±9.2
142	0.515±0.020	2.4 ±0.4	2.5 ±0.6	3.0 ±0.6	2.45±0.12	4.3±6.5
143	0.246±0.013	1.4 ±0.3	1.0 ±0.7	1.3 ±0.6	1.06±0.09	
144	0.032±0.020	0.5 ±0.4	0.6 ±0.5		(0.30)	

^aJ. Chaumont (Ref. 9).

^bB. L. Tracy *et al.* (Ref. 1).

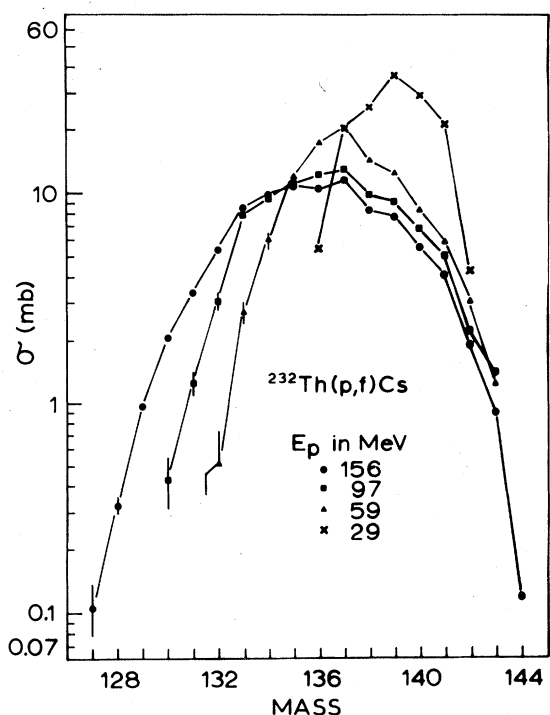


FIG. 4. Independent yields of Cs isotopes produced in the $^{232}\text{Th}(p,f)\text{Cs}$ reaction. Data for 156 MeV incident proton energies are taken from Ref. 9.

deed, the direct reaction mechanism would lead to low-excitation energy fission events that would contribute more to the Rb-Cs formation cross section than to the almost symmetric charge split leading to In. In other words, the average excitation energy of the events producing the Rb-Cs pair (asymmetric) would be lower than that of those events producing In (nearly symmetric), therefore yielding a smaller number of neutrons.

The second moment of the distribution is the variance σ^2 , which is a measure of the width of the distribution. The values of σ are given in the fourth column of Table V. It is readily apparent that the widths of the In distributions are somewhat anomalous, being closer to those of Rb whereas the mass of In is closer to Cs. The explanation might come from indium being produced in a more restricted spectrum of excitation energies and fissioning nuclei than Rb and Cs.

It has been assumed by some authors^{8,10,12} that charge distributions can be represented by Gaussian forms even at high incident proton energies. The Cs distributions obtained by mass spectrometers differ markedly from such a simple form. A quantitative way of expressing deviation from a Gaussian shape is to examine the skewness (related to the third moment) and the excess (related

TABLE V. Mass distribution statistical moments and related quantities.

Proton energy (MeV)	Centroid	$\langle N/Z \rangle$	[Second moment] ^{1/2}	Skewness	Excess
Rubidium					
156 ^a	90.00 ± 0.05	1.432 ± 0.002	2.14	-0.068	-0.099
97	90.41 ± 0.05	1.444 ± 0.002	1.95	0.022	-0.054
75	90.62 ± 0.04	1.449 ± 0.002	1.86	0.077	0.073
59	90.80 ± 0.04	1.454 ± 0.002	1.75	0.069	0.071
50 ^b	90.75 ± 0.01	1.4527 ± 0.0003	1.76	0.061	0.042
29	91.49 ± 0.04	1.473 ± 0.002	1.64	0.080	0.070
Cesium					
156 ^a	135.89 ± 0.15	1.471 ± 0.004	3.10	0.02	-0.42
97	136.71 ± 0.15	1.486 ± 0.004	2.79	0.18	-0.32
75	137.06 ± 0.15	1.492 ± 0.004	2.52	0.22	-0.27
59	137.36 ± 0.14	1.497 ± 0.004	2.23	0.28	-0.19
50 ^b	137.50 ± 0.02	1.5000 ± 0.0004	2.06	0.28	0.14
29	139.01 ± 0.22	1.527 ± 0.006	1.47		
Indium					
97	120.14 ± 0.03	1.452 ± 0.001	1.94	0.055	-0.064
75	120.46 ± 0.07	1.458 ± 0.002	1.90	0.099	0.009
59	121.03 ± 0.06	1.470 ± 0.002	1.82	0.062	0.023
48	121.57 ± 0.06	1.481 ± 0.002	1.77	0.071	0.010

^aJ. Chaumont (Ref. 9).

^bB. L. Tracy *et al.* (Ref. 1).

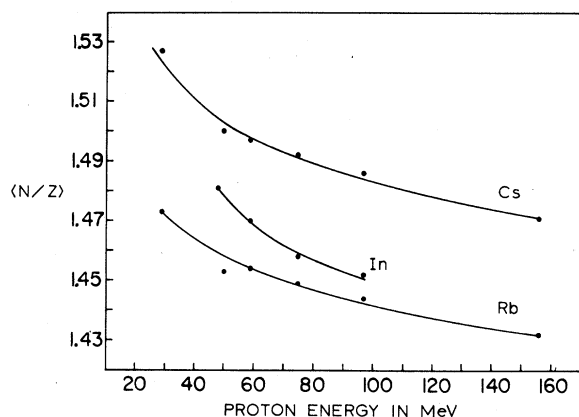


FIG. 5. Variation of neutron to proton ratio of the centroids of isotopic distributions (indicated as $\langle N/Z \rangle$) with proton energy. Data at 156 and 50 MeV energies are taken from earlier reports (Ref. 9 and 1).

to the fourth moment) of the distribution. The skewness gives the horizontal asymmetry of a distribution (a greater area on the left or right side of a distribution gives a third moment that is negative or positive, respectively) whereas the excess is negative for a distribution flattened with respect to a Gaussian and positive for a peaked distribution. Obviously, both skewness and excess are zero for a Gaussian distribution.

The excess and skewness of different isotopic distributions are given in columns 5 and 6 respectively, of Table V. It is apparent that, although the Rb distributions are well represented by Gaussian forms, the skewness and excess values of these distributions demonstrate energy dependence similar to the more asymmetric and flattened Cs distributions. It is thus seen that the mechanisms responsible for the structure observed in the Cs distributions are also at play, although less apparently, in the Rb case. A similar analysis has been done on the previously published^{1,2} isotopic distributions of Rb and Cs produced in the $^{238}\text{U}(p,f)$ reaction. Identical trends are ob-

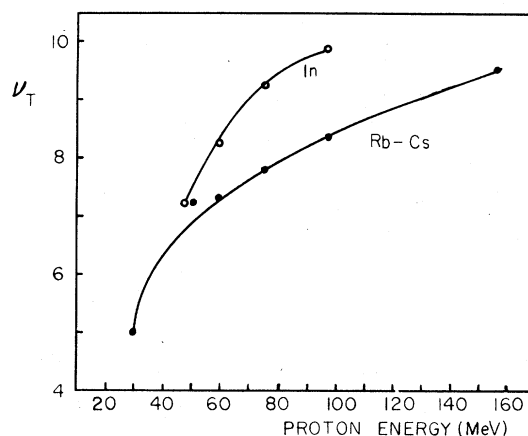


FIG. 6. Variation of total number of neutrons emitted per fission event (ν_T) with incident proton energy. The 50 and 156 MeV data are taken from Refs. 1 and 9, respectively.

served. The In distributions are found to be nearly Gaussian, at least up to 100 MeV.

C. Two-Gaussian fits to the Cs distributions

Since the asymmetric Rb-Cs split is produced in events of both high-excitation energy (like those leading to indium fragments) and low-excitation energy (that would not contribute significantly to indium), one can assume the Cs distribution to consist of two components, an indium-like component which could be well represented by a Gaussian, and another one comprising of fragments produced in the fission of nuclei with low-excitation energy. We parametrized the latter component as a second Gaussian. The validity of such an assumption is based on the fact that a Gaussian form is a good representation of the indium distribution, that the structure observed in the Cs distribution definitely looks like a shoulder on a symmetrical shape, and that one expects direct reaction events to lead to fissioning nuclei with masses close to that of the target nucleus, with rather low-excitation energies. Fission events following direct processes would lead to Cs fragments on the heavy-mass side of the distributions, where the shoulder is indeed observed. However, the possibility of a skewed Gaussian instead of two discrete overlapping Gaussians is not ruled out.

A computer program was used to decompose the Cs distributions into two Gaussians. At the lower proton energies (50, 59, and 75 MeV), a sharp minimum in the χ^2 was found with the heavier component centered around $A=140$. The analysis was less decisive for 97 MeV and 156 MeV data as the χ^2 exhibited a flat minimum with the variation of

TABLE VI. Total emitted neutrons.

Proton energy (MeV)	Rb-Cs	In
156	9.56 ± 0.16	
97	8.34 ± 0.16	9.88 ± 0.06
75	7.79 ± 0.15	9.28 ± 0.12
59	7.31 ± 0.14	8.22 ± 0.11
50	7.23 ± 0.02	
48		7.22 ± 0.12
29	5.00 ± 0.22	

the center of heavy component. The results of such an analysis gave a broad heavier component whose relative contribution increased with incident proton energy. In view of the remarkably fixed heavy-mass wing of the distribution, the 97 and 156 MeV data were fitted using the average ($A = 140.29$) heavy-mass centroid found at 50, 59, and 75 MeV. The results obtained in this analysis are presented in Table VII, and the quality of fits is shown in Fig. 7. As seen from Table VII the fixed heavy component gives a fit to the observed mass distribution with a width (FWHM) between 3.4 and 4.0 mass units which does not show any dependence on proton energy. However, the width of the lighter component increases with bombarding energy. At 29 MeV bombarding energy we observed a narrow mass distribution centered around mass 139, which is very close to the heavy-mass component (centre at $A = 140$). A visual inspection of this mass distribution does not indicate any two component structure and therefore we did not attempt a two-Gaussian fit on this spectrum. The implication is probably that, as the incident proton energy increases, a much broader range of excitation energies and fissioning nuclei are produced. The overall effect of this could lead to a broadened heavy component shifting to lighter masses. Also the possibility that a simple two-Gaussian analysis ceases to be valid at higher energies cannot be ruled out.

A possible check of this analysis can be made by calculating the total number of neutrons associated with the light component [ν_{TL}] of the Cs distribution. To obtain this quantity, one has to find the associated light Rb component, which cannot be extracted directly from the observed isotopic distribution because of the absence of a

discernible structure. An indirect manner can be found by plotting the Rb centroids versus the Cs centroids obtained at all the energies. A linear relationship is found, as shown in Fig. 8, which gives a slope of 0.5 which is related to the observed ratio of 2 between the number of neutrons emitted from Cs and those emitted from Rb.^{13,14} We obtained the centroid of the heavy Rb component associated with the heavy Cs component by using the above curve. The relative strengths of light and heavy components of Rb were taken to be the same as the corresponding quantities for Cs (since they are complementary). The total number of neutrons ν_{TL} produced in the fission events leading to the light component were calculated using Rb and Cs centroids. The results are shown on Fig. 9. The ν_{TL} values are very close to the ν_T values associated with the indium fission fragments. The relative strengths of the heavier components seem to be underestimated at 97 and 156 MeV (as indicated in the discussion of the two-Gaussian analysis).

D. Reaction mechanism: UCD versus ECD

Previous work by mass spectrometry¹⁻³ on the proton-induced fission of ²³⁸U showed that up to 100 MeV incident proton energies, the equal charge displacement (ECD) postulate was in agreement with experimental results. To obtain agreement with UCD (unchanged charge distribution), one had to make the assumption that the ratio of postfission neutrons for Rb and Cs (ν_{Cs}/ν_{Rb}) was significantly less than one, contrary to experiment. Furthermore, it was shown that this result was not sensitive to the exact value of $\nu_{\text{pre fission}}/\nu_T$. It was recently³ shown that the same conclusion is valid at 100 MeV for a more asymmetrical pair

TABLE VII. Fitting parameters for Cs mass distributions.^a

Proton energy (MeV)	a_1^b	b_1	FWHM(1) ^c	a_2	b_2	FWHM(2)
156 ^d	11.3	135.49	7.04	2.32	140.29 ^e	3.38
97	13.0	136.04	5.56	3.85	140.29 ^e	3.95
75	14.9	136.28	4.74	4.73	140.33	3.49
59	18.1	136.53	4.10	6.40	139.98	3.81
50 ^f	23.0	137.10	4.15	3.63	140.56	3.39

^a Observed mass distribution fitted to a function of the form $y = \sum_{i=1}^2 a_i e^{-(x-b_i)^2/c_i}$.

^b The values of parameters a_1 and a_2 are normalized so that the total area under the two Gaussian distributions is equal to the measured total cross section at that energy.

^c FWHM (full width at half maximum) calculated from c_i .

^d J. Chaumont (Ref. 9). The reported mass distribution was normalized to give total cross section equal to one measured at 97 MeV bombarding energy.

^e Average of b_2 for mass distributions at 75, 59, and 50 MeV.

^f B. L. Tracy *et al.* (Ref. 1).

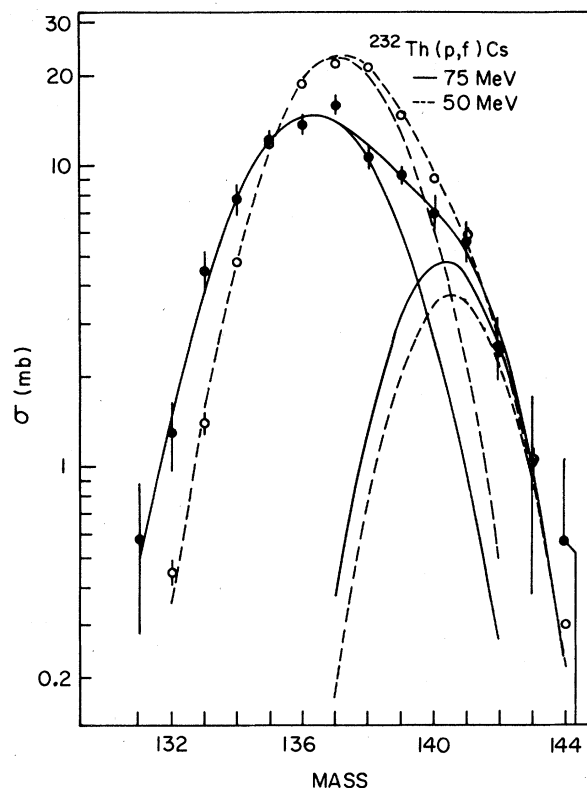


FIG. 7. Isotopic distributions of Cs isotopes fitted by using two Gaussian distributions.

Ga and Pm.

Our analysis of the $^{232}\text{Th}(p,f)$ reaction is in agreement with the preceding conclusions, as shown in Table VIII. Using the best known values^{13,14} for $\nu_{\text{prefission}}/\nu_{\text{total}}=0.5$ and $\nu_{\text{Cs}}/\nu_{\text{Rb}}=2.0$, the actual displacement $[\Delta = \langle N/Z \rangle_{\text{Cs}} - \langle N/Z \rangle_{\text{Rb}}]$ was found to be remarkably constant (-0.055) at all energies. This seems to indicate that the

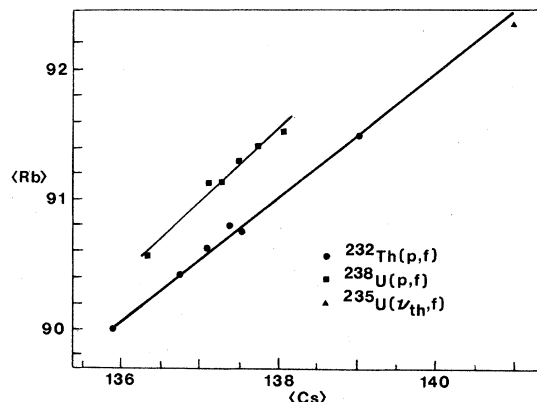


FIG. 8. Variation of the centroids of the mass distributions of Rb with those of Cs for proton-induced fission of ^{232}Th , ^{238}U , and ^{235}U .

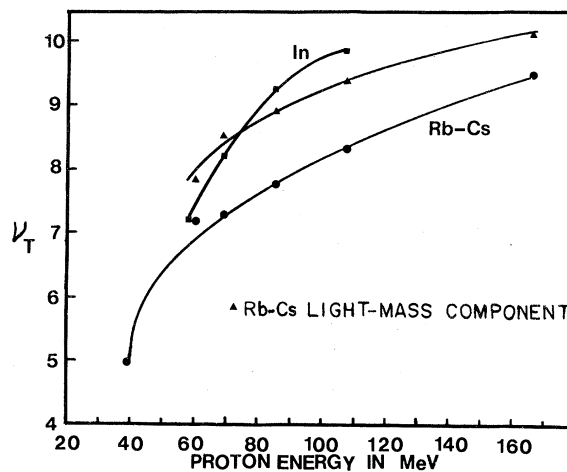


FIG. 9. Comparison of the total numbers of neutrons per fission event obtained by using the light-mass centroids of the Cs distributions with those obtained by using the centroids of the total isotopic distribution.

mechanism responsible for the charge split does not depend on excitation energy.

Previous studies by radiochemical methods^{15,16} have indicated a gradual shift towards UCD at higher incident proton energies. Our measurements do not seem to substantiate the above hypothesis. The disagreement between the results obtained by the two different methods might be due to the presence of the heavy component which cannot be observed directly by radiochemical methods (although it is accounted for indirectly by using cumulative yields to fix the heavy side of the charge distribution). It was checked whether the light-mass components of the isotopic distributions, which result from higher excitation energy events, would exhibit a UCD behavior. As shown in Table IX, one must make the improbable assumption that $\nu_H < \nu_L$ in order to obtain agreement with the UCD mechanism.

IV. CONCLUSION

In this paper, we have presented results on the proton-induced fission of ^{232}Th obtained by on-line mass spectrometry over a wide range of incident proton energies (29–97 MeV). Results on the nearly symmetric (indium) and asymmetric (Rb and Cs) fission of ^{232}Th are obtained. It has been found that the isotopic distributions of indium exhibit different characteristics than the Rb-Cs pair. In particular, more neutrons are emitted at higher proton energies from events leading to indium than from those leading to Rb and Cs. Furthermore, the indium distributions are approximated as Gaussians, whereas the Rb-Cs distributions exhibit structure on the heavy-mass side, and

TABLE VIII. A test of the validity of ECD and UCD mechanisms using the centroids of isotopic distributions. An ECD mechanism seems to be favored for the range of excitation energies studied in the present work.

Proton energy MeV	Centroids		$\frac{\nu \text{ fission}}{\nu \text{ total}}$	$\frac{\nu \text{ (Cs)}}{\nu \text{ (Rb)}}$	Deduced primary fragment mass		$\langle N/Z \rangle$		Δ^c
	$\langle \text{Rb} \rangle$	$\langle \text{Cs} \rangle$			$\langle \text{Rb}' \rangle$	$\langle \text{Cs}' \rangle$	$\langle \text{Rb}' \rangle$	$\langle \text{Cs}' \rangle$	
156 ^a	90.00	135.89	0.5	2.0	91.59	139.07	1.475	1.529	0.054
			1.0	2.0	93.18	142.26	1.518	1.587	0.069
			0.0	2.0	90.00	135.89	1.432	1.471	0.039
			0.5	0.73	92.76	137.91	1.507	1.507	0.0
97	90.41	136.71	0.5	2.0	91.80	139.49	1.481	1.536	0.055
			0.5	0.6	93.02	138.27	1.514	1.514	0.0
75	90.62	137.06	0.5	2.0	91.92	139.66	1.484	1.539	0.055
			0.5	0.55	93.13	138.44	1.517	1.517	0.0
59	90.80	137.36	0.5	2.0	92.02	139.80	1.487	1.542	0.055
			0.5	0.50	93.24	138.58	1.520	1.520	0.0
50 ^b	90.75	137.50	0.5	2.0	91.96	139.91	1.485	1.544	0.055
			0.5	0.45	93.24	138.62	1.520	1.520	0.0
29	91.49	139.01	0.5	2.0	92.32	140.68	1.495	1.558	0.063
			0.5	0.13	93.70	139.30	1.532	1.532	0.0

^a Data taken from Ref. 9.^b Data taken from Ref. 1.^c $\Delta = \langle N/Z \rangle \text{Cs}' - \langle N/Z \rangle \text{Rb}'$, $\Delta=0$ for UCD.

could be assumed to consist of two Gaussian components for Cs. It appears that the events leading to the light-mass components are similar to those leading to the production of indium as they yield almost the same number of neutrons. The observed independent yields do not seem to agree with the unchanged charge distribution (UCD) hypothesis.

It remains to understand the nature of the distinctly observed heavy-mass component in the Cs distributions. The low ν_T value associated with that component (3–3.5) indicates that the fissioning nuclei responsible for that component are close in mass to the target nucleus and have a low-excitation energy (~10–20 MeV). Over the energy range where the analysis appears to be

TABLE IX. A test of the validity of UCD and ECD mechanisms using the centroids of the light-mass components of measured isotopic distributions.

Proton energy MeV	Centroid		ν_T	$\frac{\nu \text{ fission}}{\nu \text{ total}}$	$\frac{\nu \text{ (Cs)}}{\nu \text{ (Rb)}}$	Deduced primary fragment mass		$\langle N/Z \rangle$		Δ^c
	$\langle \text{Rb} \rangle$	$\langle \text{Cs} \rangle$				$\langle \text{Rb}' \rangle$	$\langle \text{Cs}' \rangle$	$\langle \text{Rb}' \rangle$	$\langle \text{Cs}' \rangle$	
156 ^a	89.79	135.49	10.16	0.5	2.0	91.48	138.88	1.472	1.525	0.053
				1.0	2.0	93.18	142.26	1.518	1.587	0.069
				0.0	2.0	89.79	135.49	1.427	1.463	0.036
				0.5	0.78	92.64	137.72	1.504	1.504	0.0
97	90.06	136.04	9.37	0.5	2.0	91.62	139.16	1.476	1.530	0.054
				0.5	0.70	92.82	137.97	1.509	1.509	0.0
75	90.27	136.28	8.91	0.5	2.0	91.76	139.25	1.480	1.532	0.052
				0.5	0.69	92.91	138.10	1.511	1.511	0.0
59	90.38	136.53	8.55	0.5	2.0	91.80	139.38	1.481	1.534	0.053
				0.5	0.65	92.97	138.21	1.513	1.513	0.0
50 ^b	90.50	137.10	7.79	0.5	2.0	91.88	139.70	1.483	1.540	0.057
				0.5	0.53	93.13	138.45	1.517	1.517	0.0

^a Data taken from Ref. 9.^b Data taken from Ref. 1.^c $\Delta = \langle N/Z \rangle \text{Cs}' - \langle N/Z \rangle \text{Rb}'$, $\Delta=0$ for UCD.

valid, the importance of that component varies from 10 to 20%. It is tempting to believe that it represents the direct reaction contribution to the fission process, although the compound nucleus formation cross section is certainly inferior to 80% even at 80 MeV.

Another interesting observation which deserves a comment is the following. All the experiments done by on-line mass spectrometry on the proton-induced fission of the heavy elements (^{232}Th , ^{235}U , ^{238}U) over a wide range of proton energies give results which indicate that the charge division mechanism is not a function of proton energy (at least up to 156 MeV for the Rb-Cs pair and at 100 MeV for the Ga-Pm pair). However, since the postulate of ECD appears to reproduce the data well (contrary to UCD), it would be interesting to investigate physical mechanisms that can lead to the situation described by that postulate. The recent success of the two-center shell model in accounting for the long standing riddle of the two-humped fission mass distributions of the heavy elements¹⁷ encourages one to look into that direction for possible charge division mechanisms. More recently, a double core model¹⁸ for fission has been proposed. This model accounts well, at

least qualitatively, for some results on low energy fission. It states that the fragment cores are the stable isotopes for a given value of Z ; the excess neutrons are then shared equally between the two fragments. Such a model, which was originally developed to explain the fission of nuclei with low-excitation energies, is in essential agreement with ECD (although the heavier fragment should have a slightly larger number of excess neutrons in the latter hypothesis). It implies that, after the condensation of the fragment cores, the excess neutrons form the nuclear matter in the necking region. Obviously, such a model leaves much to be proven. In particular, why should the excess neutrons be shared equally between very unequal fragments? It would be of interest to investigate further the charge division mechanism over a wide range of excitation energies.

ACKNOWLEDGMENTS

The authors wish to thank Professor J. K. P. Lee for his interest in this work. Two of the authors (B.P.P. and L.L.) are grateful to Professor P. Depommier for permitting us to use the facilities at the Laboratoire de Physique Nucléaire in the preparation of this manuscript.

*Present address: Montreal Neurological Hospital and Institute, McGill University, Montreal, Quebec, Canada.

†Present address: Institute of Occupational Health and Safety, McGill University, Montreal, Quebec, Canada.

‡Present address: Laboratoire de Physique Nucléaire, Université de Montreal, Montréal, Québec, Canada.

§On sabbatical leave from the Department of Physics, Schuster Laboratory, University of Manchester, United Kingdom.

¹B. L. Tracy, J. Chaumont, R. Klapisch, J. M. Nitschke, A. M. Poskanzer, E. Roeckl, and C. Thibault, *Phys. Rev. C* **5**, 222 (1972).

²J. K. P. Lee, G. Pilar, B. L. Tracy, and L. Yaffe, *J. Inorg. Nucl. Chem.* **37**, 2035 (1975).

³K. C. Chan, B. P. Pathak, L. Nikkinen, L. Lessard, and I. S. Grant, *J. Inorg. Nucl. Chem.*, **39**, 1915 (1977).

⁴M. de Saint-Simon, L. Lessard, W. Reisdorf, L. Remsberg, C. Thibault, E. Roeckl, R. Klapisch, I. V. Kuznetsov, Yu. Ts. Oganessian, and Yu. E. Penionshkevitch, *Phys. Rev. C* **14**, 2185 (1976).

⁵W. Reisdorf, M. de Saint-Simon, L. Remsberg, L. Lessard, C. Thibault, E. Roeckl, and R. Klapisch, *Phys. Rev. C* **14**, 2189 (1976).

⁶M. Diksic, D. K. McMillan, and L. Yaffe, *J. Inorg. Nucl. Chem.* **36**, 7 (1974); H. Marshall and L. Yaffe, *ibid.* **35**, 1797 (1973); etc.

⁷P. P. Benjamin, D. A. Marsden, N. T. Porile, and L. Yaffe, *Can. J. Chem.* **47**, 301 (1969).

⁸T. McGee, C. L. Rao, and L. Yaffe, *Nucl. Phys.* **A173**, 595 (1971).

⁹J. Chaumont, Ph.D. thesis, Faculté des Sciences, Orsay, 1970 (unpublished).

¹⁰L. D. Miller and L. Yaffe, *J. Inorg. Nucl. Chem.* **35**, 1805 (1973).

¹¹L. Nikkinen, B. P. Pathak, L. Lessard, and J. K. P. Lee, *Nucl. Instrum. Methods* (in press).

¹²T. McGee, C. L. Rao, and L. Yaffe, *J. Inorg. Nucl. Chem.* **34**, 3325 (1972).

¹³E. Cheifetz, Z. Fraenkel, J. Galin, M. Lefort, J. Péter, and X. Tarrago, *Phys. Rev. C* **2**, 256 (1970).

¹⁴E. Cheifetz and Z. Fraenkel, *Phys. Rev. Lett.* **21**, 36 (1968).

¹⁵L. Yaffe, in *Proceedings of the Second International Atomic Energy Symposium on Physics and Chemistry of Fission, Vienna, Austria, 1969* (IAEA, Vienna, 1969).

¹⁶L. J. Colby, Jr. and J. W. Cobble, *Phys. Rev.* **121**, 1410 (1961).

¹⁷U. Mosel, in *Proceedings of Heavy Ion Summer Study, Oak Ridge National Laboratory Report No. CONF-720669*, 287 (1972).

¹⁸M. L. Chatterjee, *Phys. Lett.* **66B**, 319 (1977).